Biology and Fertility of Soils
https://doi.org/10.1007/s00374-022-01675-4

ORIGINAL PAPER

Absolute microbiome profiling highlights the links among microbial stability, soil health, and crop productivity under long-term sod-based rotation

Kaile Zhang[1,2] · Gabriel Maltais-Landry[2] · Michael James[2,3] · Valerie Mendez[1,2] · David Wright[1] · Sheeja George[1] · Hui-Ling Liao[1,2]

Received: 1 May 2022 / Revised: 6 October 2022 / Accepted: 7 October 2022

Abstract

High-throughput sequencing has become a critical tool for studying microbiomes by measuring relative microbiome profiling, although this typically overlooks the absolute abundance of microbiomes. Consequently, pathological, physiological, and ecological roles of microbial communities may be represented inaccurately. To address this, we estimated absolute abundances of soil microbiomes by combining amplicon sequencing with quantitative PCR. We collected soil samples (0–30 cm) at three sampling times (pre-planting, flowering, and maturity) from peanut plots subject to a long-term conventional rotation (peanut-cotton-cotton, CR) or sod-based rotation (bahiagrass-bahiagrass-peanut-cotton, SBR). Rotation and sampling time were important in shaping microbial communities. Relative to CR, SBR had greater microbial diversity, greater community stability, complexity and stability of bacterial-fungal networks, and greater richness and abundance of keystone taxa, which may make soil microbiomes more resilient to environmental changes among sampling times. SBR also showed significantly greater concentrations of total C and N, NO_3^--N, resin-extractable P, Mg, Zn, Fe, and Cu, and greater potential N mineralization rates and C:N ratios, indicating that SBR's higher rotational diversity affected soil health in the topsoil. There were more significant relationships between soil nutrients and microbial community composition as well as keystone taxa under SBR, indicating that higher rotational diversity intensified ecological connections among soil, microbes, and crops. Our results suggest that a more complex and stable microbial network with greater richness and abundance of keystone taxa (primarily bacterial communities) had critical impacts on nutrient cycling and plant health and fitness under SBR, which are the main factors contributing to crop productivity.

Keywords Estimated absolute abundances of microbiomes · Crop rotation · Perennial grass · Temporal dynamics · Bacterial-fungal networks · Microbial stability

Introduction

With an increasing global population and demand for food, agricultural systems are undergoing both expansion and intensification (Foley et al. 2011; Zhang et al. 2013). It has been demonstrated that agricultural expansion and intensification have resulted in a wide range of environmental issues, including loss of soil biodiversity, soil degradation and erosion, greenhouse gas emissions, and groundwater pollution (Tsiafouli et al. 2015; Bender et al. 2016; Campbell et al. 2017). Alternative farming systems, such as those including more diversified crop rotations, have been advocated to reduce these detrimental environmental impacts or reverse these trends without negative effects on crop productivity and soil health (Bommarco et al. 2013; Tiemann et al. 2015;

✉ Kaile Zhang
kaile.zhang@ufl.edu

✉ Gabriel Maltais-Landry
maltaislandryg@ufl.edu

[1] North Florida Research and Education Center, University of Florida, 155 Research Road, Quincy, FL 32351, USA

[2] Department of Soil, Water, and Ecosystem Sciences, University of Florida, Gainesville, FL 32611, USA

[3] Present Address: Sangre Grande 420205, Trinidad and Tobago

Published online: 21 October 2022

Zhang et al. 2021). Crop rotation increases temporal plant diversity by sequentially planting diverse crops on the same field over time. Recent studies reported that increasing the functional diversity of crops in rotation by integrating crops with diverse functional traits (e.g., cover crops and perennial crops) is a more sustainable alternative than rotating functionally similar crops to increase crop yield, as greater functional diversity can improve soil health while supporting diverse soil microbiomes (Faucon et al. 2017; Tamburini et al. 2020; Zhang et al. 2022b).

Previous studies in annual cropping systems have reported that soil microbial communities are modulated by the complex and dynamic interactions between plant growth and environmental variables (Hartman et al. 2018; Simon et al. 2020; Shen et al. 2021). For example, soil microbial community assembly is profoundly regulated by plant developmental stages (Wang et al. 2019; Geisen et al. 2021). This is partially driven by the substantial yet variable fraction (11–40%) of photosynthetically fixed C allocated belowground and subsequently exuded by plant roots, known as rhizodeposition, that has a crucial influence on soil microbiomes (Eisenhauer et al. 2017). The amount and composition of rhizodeposition are context-specific and vary with plant developmental stage and nutrition, environmental conditions, and other factors (Badri and Vivanco 2009; Steinauer et al. 2016). However, as variations in plant developmental stages are co-occurring with seasonal changes in temperature, precipitation, and radiation that also profoundly affect soil microbial communities directly (Shen et al. 2021), it is difficult to separate the effects of plant developmental stages from seasonal changes in climate conditions.

The assembly, composition, and stability of soil microbiomes are also modulated by biotic interactions (Barberán et al. 2012). Complex interactions among the myriad of microorganisms can be identified with microbial co-occurrence networks that measure the complexity and stability of microbiomes, the links between microbe-microbe interactions and ecosystem functioning, and their responses to environmental changes (Fuhrman 2009; Faust and Raes 2012; Morriën et al. 2017; de Vries et al. 2018; Banerjee et al. 2019). Still, the mechanisms driving soil microbial assembly, stability, and interactions along plant developmental stages under different long-term agricultural practices remain largely unknown. This knowledge gap is critical given that a better understanding of temporal dynamics in soil microbial assembly, interactions, and functions could help develop microbial-based approaches for sustainable agriculture (Haskett et al. 2020; D'Hondt et al. 2021).

Given the tight association between soil microbiomes and microbial functioning, changes in soil microbial communities significantly affect the availability of C and nutrients in addition to soil health (Paul 2014; Crowther et al. 2019). Soil chemical properties that can be quantified rapidly and are responsive to changes in agricultural management are often used to determine the effects of soil microbiomes on nutrient availability and soil health, such as permanganate oxidizable C (POXC), soil protein, and Mehlich-extracted elements (Hurisso et al. 2018a). For example, POXC serves as a reservoir of biologically available C, including microbial biomass, that is sensitive to agricultural management (Culman et al. 2012). Soil protein is an operationally defined soil N pool that is used as an indicator of mineralizable N and estimates the amount of soil organic matter compounds containing organic N (Nannipieri and Paul 2009). Soil protein was found to show a strong response to management practices such as tillage and rotational diversity (Moebius-Clune et al. 2008; Hurisso et al. 2018b). As soil nutrient availability affects plant performance directly (Berendsen et al. 2012), measuring the temporal variability in nutrient availability across plant developmental stages and seasonal changes in climate can help better understand the linkages among soil microbiomes, soil health, and crop productivity.

With the rapid advancement in omics techniques, such as high-throughput molecular technologies, affordable amplicon sequencing has been widely adopted to analyze microbial community profiling (Almeida and Shao 2018). Although this method provides important insights into the diversity and composition of microbial communities, it is inherently limited by the fact that it calculates the relative abundance of taxa rather than the actual abundance of the population (Widder et al. 2016). Props et al. (2017) reported that the relative abundance of a taxon and its absolute abundance were not necessarily related. It is possible that a microbial group could show an upward trend in absolute abundance while decreasing relative abundance in a given environment, and vice-versa. In this scenario, relative microbiome profiling may mask the underlying pathological, physiological, and ecological roles of microbial communities (Tkacz et al. 2018), as these are typically driven by the absolute abundance of soil microbes. Accordingly, without absolute microbiome profiling (AMP), it is difficult to systematically and holistically understand the spatio-temporal dynamics of microbial abundance and how microbes affect ecosystem functions, in addition to their responses to environmental changes and anthropogenic disturbances (Tkacz et al. 2018; Guo et al. 2020b; Tettamanti Boshier et al. 2020). Thus, quantifying absolute abundances of microbial communities should improve our ability to determine the extent to which soil microbiomes affect nutrient dynamics and further contribute to crop performance and productivity in agroecosystems.

In this study, we determined the relative and estimated absolute abundances of soil microbial communities using amplicon sequencing and quantitative PCR (qPCR), respectively, in agroecosystems with different crop rotation systems and irrigation

regimes. Our main objectives were to (1) compare AMP and microbial community stability under different irrigation regimes and crop rotation systems at various sampling times; (2) uncover the temporal dynamics of bacterial-fungal networks and their ecological roles in different crop rotation systems; and (3) identify the mechanisms through which soil microbial communities affect soil health and crop performance and productivity under different crop rotation systems. We hypothesized that (1) sampling time would have stronger effects on soil microbial communities under conventional rotation (peanut-cotton-cotton, CR) relative to sod-based rotation (bahiagrass-bahiagrass-peanut-cotton, SBR); (2) SBR would enhance the complexity of soil microbial networks and associated agroecosystem functions across different sampling times; and (3) SBR would improve soil health and crop productivity by assembling more diverse and abundant keystone taxa compared to CR.

Materials and methods

Experiment site and design

This field trial was initiated in 2000 at the North Florida Research and Education Center, Quincy, Florida (30° 32.79' N, 84° 35.50' W), on a soil mapped as a Dothan sandy loam (fine-loamy, kaolinitic, thermic Plinthic Kandiudult) (Zhao et al. 2010). The experiment compares two rotation systems: a peanut (*Arachis hypogaea* L. cv. Georgia Green)-cotton (*Gossypium hirsutum* L. cv. Deltapine® 1646)-cotton rotation (conventional rotation, CR) and a bahiagrass (*Paspalum notatum* Flugge cv. Pensacola)-bahiagrass-peanut-cotton rotation (sod-based rotation, SBR). Each crop phase within these two rotations is considered as a treatment; there are therefore three crop treatments for CR and four crop treatments for SBR. An oat (*Avena sativa* L. cv. Florida 501) cover crop is planted after harvesting cotton and peanut in both rotations as well as after the second year of bahiagrass in SBR. The study is set up as a randomized complete block design combined with a split-plot arrangement. All crop phases of two rotations (main plots) are presented each year in each of three blocks, in 128×45.7 m^2 plots, with irrigated (irrigation and precipitation) and rainfed (precipitation only) treatments (split plots). Irrigated split plots received 3 cm of water every week. All crops were planted using conservation tillage (strip tillage). Additional details of field setup, fertilization, and site maintenance can be found in Zhang et al. (2022b).

Weather data (soil temperature, precipitation, and solar radiation) were exported from the Florida Automated Weather Network (https://fawn.ifas.ufl.edu/) that maintains a weather station at the experimental site and are shown in Table S1.

Soil and peanut sample collection

Peanut (cv. Georgia Green) was seeded with a row spacing of 91 cm and depth of 2.5 cm at 20 seeds m^{-1} on 9 May 2019. Soil samples (0–30 cm depth) were collected from the two center rows of each subplot (roughly 8 cm away from plants) using an Oakfield tube at pre-planting (19 January for soil chemical properties vs. 18 March for soil microbial analyses), flowering (21 June), and maturity (5 October) stages during the 2019 growing season. Twelve soil cores (diameter = 2 cm) were collected per subplot and mixed to get a composite soil sample. In total, there were 36 samples (2 peanut phases × 2 irrigation conditions × 3 sampling times × 3 replicates). A subsample was kept at 4 °C until analysis for soil chemical properties, whereas another subsample was sieved through a screen with 0.64-cm apertures and then transferred to 2-ml Eppendorf tubes before storage at − 80 °C for microbial analyses.

Peanut was harvested on 6 October (optimum pod maturity) using a 5000 Express peanut picker (Gregory Manufacturing Co., Lewiston Woodville, NC) from the designated harvest rows of each subplot. After fresh peanuts were weighed (two weights per subplot), pod sub-samples from each subplot were placed in a forced-air dryer at 45 °C for 72 h. Final peanut yields are reported on a dry weight basis adjusted to 10% moisture.

Soil chemical properties

Within 72 h of collection, fresh soils were extracted for N and P. A laboratory incubation was used to determine potential N mineralization (PNM). Specifically, 8 g of field-moist soil from each plot was incubated in an incubator for 28 days (Allar and Maltais-Landry 2022), using an incubation temperature that matched the soil temperature observed at the field site (Table S1). Before incubation, sample moisture was adjusted to 20% of total weight using double-distilled water, and moisture adjustments were performed weekly. Soil extractable NH_4^+–N and NO_3^-–N before and after incubation were extracted with 2.0 M KCl using a 1:5 (w/v) soil-to-solution ratio (Kemmitt et al. 2005) and then analyzed for NH_4^+–N (Weatherburn 1967) and NO_3^-–N (Doane and Horwáth 2003) by colorimetry using an Epoch 2 microplate reader (Biotek, Winooski, VT). PNM was calculated according to this formula:

$$\mathrm{PNM}\left(\mathrm{mg\ N\ kg^{-1}d^{-1}}\right) = \left(\left(\mathrm{NH_4^+ - N + NO_3^- - N}\right)_{\mathrm{final}} - \left(\mathrm{NH_4^+ - N + NO_3^- - N}\right)_{\mathrm{initial}}\right) / 28\ \mathrm{days}$$

Resin-extractable P of fresh soil samples was measured using anion-exchange resins (Tiessen and Moir 2007). Briefly, 2.5 g of soil samples was extracted with moist resin strips saturated with $NaHCO_3$ and 35 mL of double distilled water on a

reciprocal shaker for 16 h. After shaking, P was eluted from the resin using 0.5 M HCl for 1 h, and P concentration was determined by colorimetry using the molybdate blue method (Tiessen and Moir 2007).

After samples were processed for extractable N and P on fresh soils, the remaining soil samples were air-dried and sieved to 2 mm. Autoclaved Citrate-Extractable soil protein and soil permanganate oxidizable C (POXC) were determined using the methods of Hurisso et al. (2018a). A soil subsample was sent to Waters Agricultural Laboratories, Camilla, Georgia, USA, for analysis of soil pH (1:1 soil-to-water ratio), total C (TC) and total N (TN) with a LECO EPS-2000 CNS thermal combustion furnace (LECO Corp., St Jose, MI, USA), and soil elements (P, K, Ca, Mg, S, B, Zn, Mn, Fe, and Cu) with Mehlich III extraction (M3) (Mehlich 1984) and quantification by inductively coupled plasma spectrometry (Agilent 157 5110 ICP-OES).

DNA extraction and quantitative PCR

Soil DNA was extracted from 0.5 g soil using the DNA PowerSoil kit (MoBio, Carlsbad, California, USA) following the manufacturer's instructions. Before the DNA concentration of each sample was assessed by spectrophotometry (NanoDrop™, Thermo Fisher Scientific, Thermo Scientific™), extracted DNA samples were cleaned up using AMPure XP beads to remove contaminants, including PCR inhibitors. After diluting DNA samples ten times, the absolute abundance of bacteria and fungi was determined on the Bio-Rad CFX96 Real-Time System (Bio-Rad Laboratories, Inc., California, USA) using primer sets 341F/806R and ITS1F/ITS4, respectively (Brabcová et al. 2016; Trivedi et al. 2016). Each reaction contained 10 µl mixture, including 5 µl SsoAdvanced Universal SYBR Green Supermix (2X), 0.3 µl (10 µM) forward and reverse primers, 1 µl DNA template, and 3.4 µl nuclease-free H_2O. Thermal cycling conditions were as follows: 30 s at 98 °C, then 40 cycles (to completely detect absolute microbial abundance) of 98 °C for 15 s and 60 °C for 30 s. Melting curve analysis was performed at the end of each real-time quantitative PCR (qPCR) by increasing temperature from 65 to 95 °C at 0.1 °C s^{-1} to check the specificity of amplification products. Amplification efficiency was calculated based on the slopes of individual amplification plots to check for PCR inhibition. All samples and calibration reactions were run with three technical replicates that showed high reproducibility and low variability among technical replicates.

Sequencing for soil microbial communities and bioinformatics

The V3-V4 region of bacterial 16S rRNA gene (341F/806R primer mixture) and the ITS1-ITS2 region of fungal ITS gene (ITS1/ITS4 primer mixture) were amplified using a modified two-step PCR on a C1000 Touch™ Thermal Cycler (Bio-Rad, Oxfordshire, UK) (Chen et al. 2021). Reverse primers were tagged with sample-specific 10-bp barcode oligonucleotides to distinguish the amplicons from different samples. All products from each PCR step were purified with the bead-cleanup approach (AMPure-XP, Beckman Instruments, Brea, CA, USA). To alleviate the sequencing bias caused by added primers and sequencing adaptors, we set 15 PCR cycles for each of our two-step PCR. The quantity and quality of final PCR products were determined by a NanoDrop spectrophotometer (NanoDrop™, Thermo Fisher Scientific, Thermo Scientific™, Wilmington, DE, USA) and screening using 1% (w/v) agarose gels, respectively. During each step, we used negative controls (i.e., nuclease-free water) to confirm that there was no contamination present. After all amplicons were pooled in equimolar concentrations (10 ng μl^{-1}) in a single tube, the mixture was sequenced on an Illumina (Illumina Inc., San Diego, CA, USA) Miseq instrument (v3 300 bp, 13 Gb sequencing capacity) at the Duke Center for Genomic and Computational Biology. The raw sequence data were deposited in the NCBI Sequence Read Archive under Study PRJNA815056.

16S and ITS raw sequences were processed using Quantitative Insights into Microbial Ecology (QIIME) 2.0 standard operation procedure (Bolyen et al. 2019). Low-quality sequences (Phred quality score $Q < 20$ or a length shorter than 220 bp) were discarded using "*data2.py*" after removing barcodes from each sample. The remaining high-quality sequences were clustered into operational taxonomic units (OTUs) at 99% identity using "*vsearch.py*". Bacterial and fungal OTUs were taxonomically assigned with Greengenes (Version 2018) and UNITE databases (Version 8) with a confidence value greater than 0.7, respectively, using "*feature-classifier.py*". Overall, 4,113,626 (mean of 114,267 per sample) bacterial and 3,212,172 (mean of 89,227 per sample) fungal high-quality reads were obtained and assigned to 14,629 and 5,377 OTUs, respectively. The estimated absolute abundance of each OTU within each sample was calculated as the product of its relative abundance and the total absolute 16S/ITS gene copy numbers based on the conclusion of Zhang et al. (2022c), who found that this method has higher stability and technical feasibility compared to the spike-in method. Finally, OTUs that were assigned to chloroplast, mitochondrial, and viridiplantae in the bacterial OTU table in addition to unidentified sequences in both bacterial and fungal OTU tables were removed.

Network analysis

Microbial co-occurrence networks were constructed using Spearman correlations (package: *psych*, function: *corr.test*) in R (version 4.0) (Hector 2015; Xia et al. 2018).

Robust correlations were selected using a threshold of $r > |0.77|$ and P value < 0.05, after adjustments with the Benjamini–Hochberg procedure to reduce the occurrence of false-positive results (Benjamini and Hochberg 1995). Networks were visualized in the Gephi software (Bastian et al. 2009). More complex soil networks were defined to have a greater number of nodes and edges, average degree, clustering coefficient (the degree of a node closely connected with neighboring ones), and closeness centrality (the central importance of a node in disseminating information), but lower values for betweenness centrality (the number of times a node acts as a bridge along the shortest path between two other nodes) and average path length (Qiu et al. 2021; Jiao et al. 2022). Nodes with either a high value of Zi ($|Zi| > 2.5$) or Pi ($|Pi| > 0.62$) were considered as potential keystone taxa given their critical role in network topology (Shi et al. 2016). The traits of keystone taxa were predicted by FAPROTAX for bacterial nodes (Louca et al. 2016) and FungalTraits for fungal nodes (Põlme et al. 2020). Linear regression models were performed to test the relationships between the abundance of keystone taxa and nutrient dynamics, and P values were adjusted by the Bonferroni-Holm method in R.

Statistical analyses

All statistical analyses were performed in R (version 4.0). After the estimated abundance of bacterial and fungal OTUs was rarefied based on the lowest abundance across all samples (11,008,350 copies for bacteria, 17,031,060 copies for fungi), the alpha diversity of bacterial and fungal communities was calculated with the Shannon index (package: *vegan*, function: *diversity*). Dissimilarities among treatments (beta diversity) were visualized using a principal coordinate analysis (PCoA) with Bray–Curtis dissimilarity distances (package: *vegan*, function: *monoMDS*) (Zhang et al. 2017, 2020a). Permutation multivariate analysis of variance (PERMANOVA) was used to assess the effects of irrigation, rotation, and sampling time on soil bacterial and fungal community composition (package: *vegan*, function: *adonis*). A partial Mantel test based on 999 permutations was performed to test the effects of weather variables and soil properties on the diversity and composition of microbial communities (package: *vegan*, function: *mantel.partial*). The average variation degree (AVD) method was applied to calculate the degree of deviation in the abundance of normally distributed OTUs across replicated soil samples (Xun et al. 2021), and we used the stability index (1-AVD) to represent soil microbial community stability. The main soil chemical and weather predictors for microbial community stability were identified with a Random Forest analysis (Trivedi et al. 2016). Percentage of increases in the mean squared error (MSE) for each variable was used to identify the importance of each predictor; higher values of MSE% indicate a more important variable (Breiman 2001). The significance of the model was evaluated with 5000 permutations of the response variable (package: *A3*; function: *a3*) (Fortmann-Roe and Others 2015).

A three-way ANOVA was used to examine the effect of irrigation, rotation, and sampling time on microbial alpha diversity, microbial abundance, stability index of microbial communities, and soil chemical properties. Shapiro–Wilk (package: *dplyr*, function: *shapiro.test*) and Levene (package: *car*, function: *levene.test*) tests were used to verify the normality of residuals and homogeneity of variance for each variable, respectively (Gastwirth et al. 2009; Hanusz and Tarasińska 2015). Variables where assumptions of normality were violated were log-transformed to achieve normality. If the interaction (i.e., rotation by sampling time or irrigation by sampling time) in the ANOVA was significant, significant differences among sampling times within the irrigated/rainfed condition or the CR/SBR rotation were determined using a Tukey's HSD test (package: *agricolae*, function: *HSD.test*), and rotation/irrigation effects for each sampling time were determined with a *t*-test. If the main effects (i.e., rotation and sampling time) were significant, differences between CR and SBR were determined with a *t*-test after pooling irrigation and sampling times, and differences among sampling times were determined using a one-way ANOVA followed by a Tukey HSD post hoc test after pooling irrigation and rotation. All results were considered significant when $P < 0.05$, while results with $0.05 < P < 0.1$ were considered as "marginally significant".

Partial least squares path modeling (PLS-PM) was used to evaluate cascading relationships among irrigation, weather changes, microbial attributes (abundance, diversity, composition, and community stability), microbial networks (complexity and keystone taxa), soil chemical properties, and peanut yield under different rotation systems (Barberán et al. 2014). PLS-PM is a powerful statistical tool that is applied in non-normally distributed data with a small sample size to study cause and effect relationships between manifest and latent variables (Tenenhaus et al. 2005; Barberán et al. 2014). The description of manifest and latent variables and the construction of models are detailed in the supplementary information (Supplementary information – Methods). After constructing several conceptual models with latent and manifest variables (package: *plspm*, function: *plspm*), the optimal model was determined to be the model with the highest determination coefficient ($R^2 > 0.60$), goodness of fit index (GoF > 0.50), and redundancy index (Mean Redundancy > 0.60) after 1000 bootstraps (Trivedi et al. 2016).

Results

Weather and edaphic properties at different sampling times

Mean soil temperature (27.3 °C) and total precipitation (18.2 cm) were highest at maturity, followed by flowering (24.5 °C and 13.2 cm) and pre-planting (17.2 °C and 7.3 cm; Table S1). However, mean solar radiation was highest at flowering (242.7 w/m^2) and lowest at pre-planting (189.6 w/m^2). Most soil chemical properties were affected by sampling time, rotation, and/or their interaction (Tables 1 and S2). For example, under CR, POXC, C:N, NO_3^-–N, protein, and resin P were lowest at pre-planting and peaked at flowering. The same trend was found for NO_3^-–N under SBR, while concentrations of POXC and resin P, as well as C:N ratio, peaked at maturity instead of flowering; there was no significant effect of sampling time for protein in SBR. We also found significantly higher POXC and resin P under CR than SBR at flowering, whereas protein (pre-planting), NO_3^-–N (flowering), and C:N (maturity) were higher under SBR than CR. In addition, TC, PNM, M3 Zn, and Fe were higher while M3 K and Mn were lower under SBR relative to CR irrespective of sampling time. Sampling time significantly affected several variables ($P < 0.05$): M3 S, B, and Zn were highest at pre-planting; M3 P, K, Mn, Fe, and Cu were highest at flowering; and PNM was highest at maturity. Compared to rotation and sampling time, irrigation only had a marginally significant interaction with rotation for M3 K and a significant main effect for TN (Table S2).

Microbial abundance, diversity, and community composition in the soil

Sampling time had a significant main effect on the estimated absolute abundance of bacteria, with greater absolute bacterial abundance at maturity relative to pre-planting

Table 1 Soil chemical properties (mean ± standard error) under different sampling times and rotations

	Pre-planting		Flowering		Maturity		ANOVA
	CR	SBR	CR	SBR	CR	SBR	
pH	6.0 ± 0.1	6.0 ± 0.1	5.8 ± 0.1	5.8 ± 0.1	5.9 ± 0.1	5.9 ± 0.1	N.S
POXC (mg kg^{-1})	220 ± 14^{c}	198 ± 19^{B}	**381 ± 21^{a}**	**236 ± 15^{AB}**	272 ± 24^{b}	246 ± 6^{A}	Time × rotation***
TC (%)	**1.10 ± 0.04**	**1.18 ± 0.06**	**1.21 ± 0.02**	**1.26 ± 0.05**	**1.13 ± 0.02**	**1.29 ± 0.03**	Rotation***
TN (%)	0.22 ± 0.01	0.23 ± 0.01^{A}	0.23 ± 0.01	0.24 ± 0.01^{A}	0.22 ± 0.01	0.21 ± 0.01^{B}	Time × rotation†
C:N	4.9 ± 0.1	5.1 ± 0.3^{B}	5.3 ± 0.2	5.4 ± 0.1^{B}	**5.1 ± 0.12**	**6.2 ± 0.1^{A}**	Time × rotation*
PNM (mg kg^{-1} d^{-1})	**-0.02 ± 0.01**	**-0.02 ± 0.01**	**0.06 ± 0.11**	**0.35 ± 0.02**	**0.17 ± 0.01**	**0.32 ± 0.02**	Time**; rotation*
NH_4^+ -N (mg kg^{-1})	0.4 ± 0.1	0.7 ± 0.1	0.5 ± 0.1	0.1 + 0.02	0.3 ± 0.1	0.4 ± 0.1	N.S
NO_3^--N (mg kg^{-1})	0.1^{b}	0.6 ± 0.1^{C}	**11.0 ± 2.0^{a}**	**19.4 ± 0.9^{A}**	7.0 ± 0.3^{a}	10.0 ± 1.4^{B}	Time × rotation *
Protein (mg kg^{-1})	**1721 ± 108^{b}**	**2393 ± 201**	2905 ± 148^{a}	2693 ± 81	2739 ± 137^{a}	2566 ± 65	Time × rotation**
Resin P (mg kg^{-1})	3.2 ± 0.8^{c}	5.4 ± 1.1^{B}	**13.8 ± 1.8^{a}**	**8.8 ± 0.8^{AB}**	9.0 ± 1.3^{b}	9.9 ± 0.6^{A}	Time × rotation**
M3 P (mg kg^{-1})	28 ± 3	30 ± 6	45 ± 5	41 ± 2	35 ± 1	36 ± 2	Time**
M3 K (mg kg^{-1})	**134 ± 7**	**100 ± 12**	**144 ± 5**	**116 ± 10**	**122 ± 6**	**90 ± 5**	Time*; rotation***
M3 Ca (mg kg^{-1})	701 ± 70	644 ± 23	630 ± 27	674 ± 39	624 ± 40	646 ± 17	N.S
M3 Na (mg kg^{-1})	5.9 ± 0.3	5.8 ± 0.2	7.3 ± 0.8	7.8 ± 1.5	6.8 ± 0.6	6.1 ± 0.2	N.S
M3 Mg (mg kg^{-1})	**129 ± 7**	**131 ± 11**	**112 ± 11**	**128 ± 4**	**121 ± 10**	**131 ± 4**	Rotation†
M3 S (mg kg^{-1})	28 ± 5	20 ± 2	15 ± 1	14	15 ± 3	12 ± 1	Time**
M3 B (mg kg^{-1})	0.3 ± 0.01	0.3 ± 0.01	0.2 ± 0.02	0.2 ± 0.01	0.2 ± 0.02	0.2 ± 0.01	Time*
M3 Zn (mg kg^{-1})	**5.5 ± 1.1**	**6.8 ± 0.4**	**2.7 ± 0.4**	**3.9 ± 0.6**	**1.6 ± 0.3**	**2.7 ± 0.2**	Time***; rotation*
M3 Mn (mg kg^{-1})	**36 ± 3**	**29 ± 2**	**41 ± 2**	**38 ± 2**	**40 ± 1**	**33 ± 2**	Time**; rotation**
M3 Fe (mg kg^{-1})	**54 ± 4**	**64 ± 6**	**69 ± 4**	**77 ± 3**	**66 ± 2**	**70 ± 2**	Time**; rotation*
M3 Cu (mg kg^{-1})	0.2 ± 0.02	0.2 ± 0.02	3.6 ± 1.0	6.1 ± 1.5	0.2 ± 0.05	0.2 ± 0.01	Time***
CEC (meq/100 g)	8.2 ± 0.3	7.8 ± 0.1	7.4 ± 0.2	8.0 ± 02	7.7 ± 0.2	7.9 ± 0.2	N.S
BS (%)	60 ± 3	59 ± 2	60 ± 2	59 ± 3	58 ± 3	58 ± 1	N.S

POXC, permanganate oxidizable C; *TC*, total C; *TN*, total N; *PNM*, potential N mineralization rate; *M3*, extracted with Mehlich III; *CEC*, cation exchange capacity; *BS*, base saturation. Lowercase and uppercase letters indicate a significant difference among developmental stages under CR and SBR, respectively, determined by a Tukey's HSD test. Values marked in bold show a significant difference between CR and SBR within each sampling point, determined by a *t*-test. ***, **, *, and † represent the significance at $P < 0.001$, 0.01, 0.05, and 0.1, respectively. N.S. indicates no significant effects. Statistical analysis of soil properties is shown in Table S3

and flowering (three-way ANOVA; $P < 0.001$; Fig. S1A; Table S3). There was a marginally significant interaction of irrigation by sampling time on absolute fungal abundance ($P = 0.07$; Fig. S1B; Table S3). Absolute fungal abundance was significantly greater at maturity compared to other sampling times under rainfed conditions ($P < 0.05$), whereas there was no difference among sampling times under irrigated conditions. In addition, absolute fungal abundance was greater in rainfed conditions ($P < 0.05$) at maturity but unaffected by irrigation at other sampling times. However, there was no significant effect of rotation on absolute abundance of bacteria and fungi (Figs. S1A and B; Table S3). By combining amplicon sequencing with qPCR, we determined the estimated absolute abundance of microbial taxa (Figs. 1A and B). Among the top 15 microbial classes, Alphaproteobacteria and Bacilli were the most dominant bacterial groups, with over 1.2×10^7 copies g^{-1} soil, while the most dominant fungal taxa were Sordariomycetes (5.1×10^7 copies g^{-1} soil) and Dothideomycetes (2.4×10^7 copies g^{-1} soil) across all samples.

The bacterial Shannon index was significantly greater at pre-planting and flowering than at maturity, and rotation had a significant main effect for both bacterial and fungal alpha diversity ($P < 0.05$), with significantly greater microbial alpha diversity in SBR compared to CR (Figs. 1C and D; Table S3).

PCoA plots of Bray–Curtis distances and PERMANOVA analyses revealed that irrigation, rotation, and sampling time significantly affected bacterial community composition ($P < 0.05$), with no significant interactions (Table 2; Fig. 1E). Compared to irrigation ($R^2 = 0.05$), rotation ($R^2 = 0.09$) and sampling time ($R^2 = 0.10$) had stronger effects on bacterial community composition, although all these effects were relatively weak (Table 2). In contrast, fungal community composition was significantly affected by sampling time and rotation ($P < 0.001$; Table 2; Fig. 1F), with a marginally significant interaction between these two factors ($P = 0.09$). Both factors ($R^2 \sim 0.15$) had similar effects on fungal community composition, and a stronger impact on fungal relative to bacterial community composition.

The effects of environmental factors on soil microbial communities

Given that weather variables and most soil chemical properties varied in response to sampling time and/or rotation, we used a partial Mantel test to identify the main variables driving the variation in microbial community composition and diversity (Figs. 2A and B). Weather variables (i.e., mean soil temperature, total precipitation, and mean radiation) significantly affected both bacterial and fungal community composition under CR ($P < 0.05$; Fig. 2A), whereas only bacterial community composition was significantly affected by mean soil temperatures and total precipitation under SBR (Fig. 2B). In CR (Fig. 2A), NO_3^-–N, protein, and M3 Zn induced significant changes in bacterial and fungal community composition, whereas TN and M3 S affected only bacterial and fungal community composition, respectively. In contrast, bacterial and fungal diversity were only associated with TN and M3 Na, respectively. Under SBR (Fig. 2B), a greater number of soil chemical properties had significant links to both bacterial and fungal community composition (TN, M3 K, B, and Zn), only bacterial community composition (POXC, TC, NO_3^-–N, protein, resin P, M3 Mg and Fe), or only soil fungal community composition (M3 S). Permanganate oxidizable C and resin P were associated with bacterial diversity, whereas no chemical properties were linked to fungal diversity in SBR. Compared to microbial community composition, microbial diversity had fewer links with soil chemical properties, irrespective of rotation systems.

Microbial co-occurrence network and keystone taxa

Bacterial and fungal co-occurrence networks were constructed based on Spearman correlations among OTUs to investigate microbial inter-connections at different sampling times under CR and SBR, respectively (Fig. 3A). We found that rotation strongly affected the topological properties of bacterial-fungal co-occurrence patterns. Specifically, SBR showed a significantly greater average degree, clustering coefficient, and closeness centrality, but lower betweenness centrality than CR across all sampling times ($P < 0.05$; Figs. 3B–E), suggesting that SBR led to a more complex soil microbial community than CR. SBR had a greater number of edges between bacteria and fungi and a lower percentage of positive correlations than CR at each sampling time, especially at flowering and maturity (Table 3). Similarly, sampling time affected multiple topological properties of bacterial and fungal co-occurrence patterns (Table 3). For example, total number of nodes and bacterial nodes, edges within bacteria, average degree, and modularity were highest at maturity, irrespective of rotation systems.

According to within-module connectivity (*Zi*) and among-module connectivity (*Pi*), nodes played a different role in bacterial and fungal networks at different sampling times (Fig. S2). Under CR, we detected the following module hubs, which represent keystone taxa: 8 at pre-planting (6 bacterial and 2 fungal nodes), 7 at flowering (5 bacterial and 2 fungal nodes), and 17 at maturity (15 bacterial and 2 fungal nodes) (Fig. 4A). In SBR, there was 5 (3 bacterial and 2 fungal nodes), 23 (18 bacterial and 5 fungal nodes), and 15 (14 bacterial and 1 fungal nodes) module hubs at pre-planting, flowering, and maturity, respectively (Fig. 4B). Although CR had a slightly greater number of keystone OTUs at pre-planting and maturity, the cumulative estimated absolute abundance of keystone taxa was greater in SBR at flowering and maturity (Figs. S3A and B).

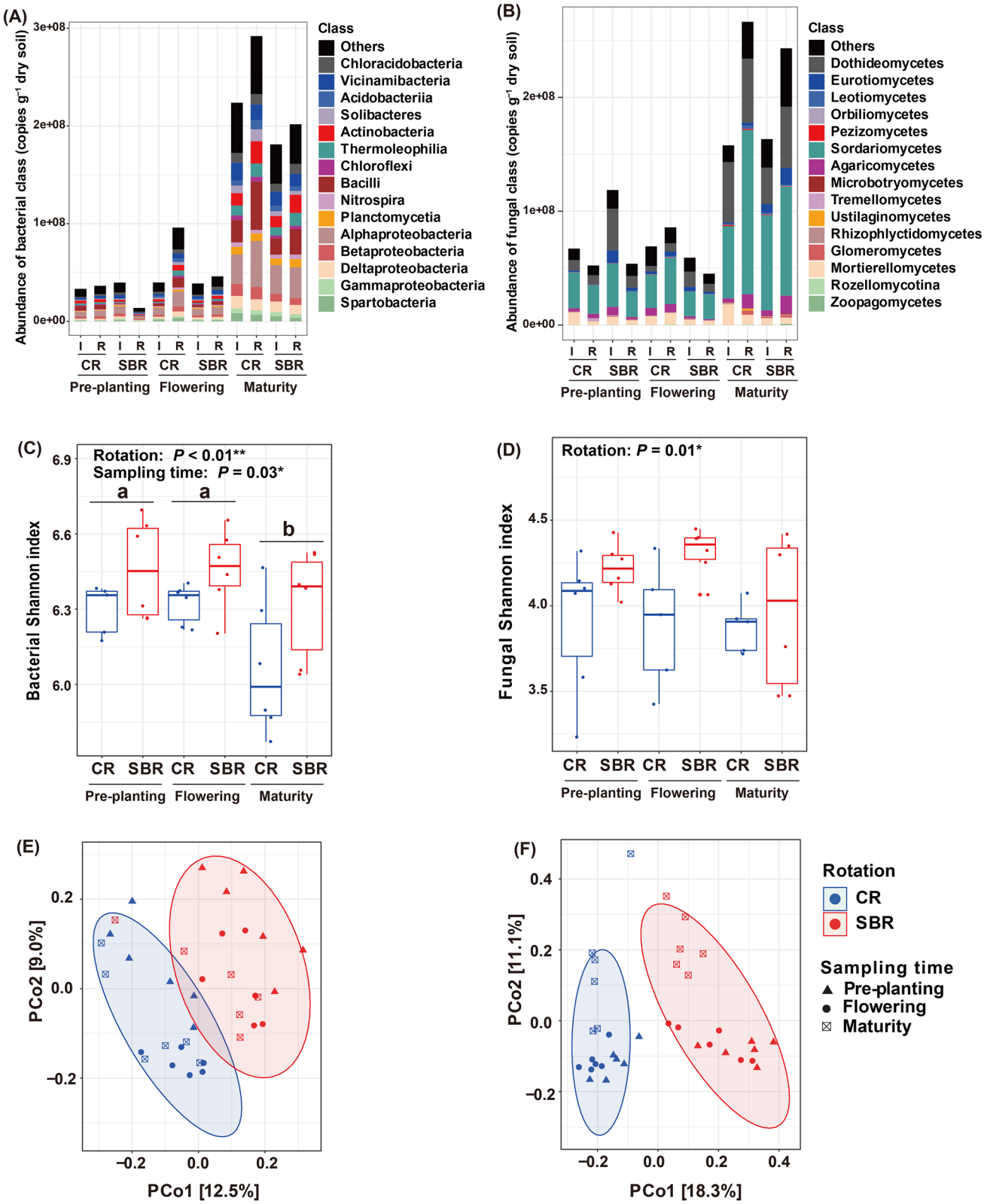

Furthermore, keystone taxa were assigned to more microbial phyla and genera in SBR (12 phyla and 34 genera) than CR (10 phyla and 23 genera; Figs. S3A and B).

As keystone taxa in SBR were predicted to be involved in C and nutrient cycling (e.g., N, S, and Fe; Fig. S3C), linear models were developed to determine the association between

◂**Fig. 1** Abundance, diversity, and composition of microbial communities: estimated absolute abundance of the top 15 bacterial (**A**) and fungal (**B**) microbial classes; bacterial (**C**) and fungal (**D**) alpha diversity measured by the Shannon index; bacterial (**E**) and fungal (**F**) beta diversity calculated with a PCoA of Bray–Curtis distance among treatments (CR, conventional rotation; SBR, sod-based rotation; I, irrigated; R, rainfed). In C, D, lowercase letters above boxes indicate significant differences among sampling times using a one-way ANOVA followed by a Tukey's HSD test for post hoc comparisons ($P < 0.05$), irrespective of irrigation and rotation. Statistical analysis for microbial alpha diversity is shown in Table S3. In E, F, ellipses include 95% confidence intervals for each rotation system (blue for CR, red for SBR). *, **, and *** indicate significance at $P < 0.05$, 0.01, and 0.001, respectively

the abundance of keystone taxa and soil chemical properties (Fig. S3D). The abundance of keystone taxa under SBR was positively related to POXC, C:N ratio, NO_3^-–N, and resin P (Figs. 4C to 4G; $R^2 = 0.25$ to 0.40, $P = 0.007$ to 0.041), but negatively related to M3 S, B, and Zn (Figs. 4H to 4J; $R^2 = 0.29$ to 0.65, $P < 0.001$ to $P = 0.032$). In CR, only PNM was significantly and positively related to the abundance of keystone taxa (Fig. 4F; $R^2 = 0.28$, $P = 0.02$).

Microbial community stability

The stability index of bacterial communities was significantly affected by the sampling time by rotation interaction (Fig. 5A; Table S3; $P < 0.05$). The stability index of bacterial communities was highest at pre-planting and lowest at maturity under SBR, but there was no significant difference through time in CR (Fig. 5A). In addition, SBR had a significantly greater stability index of bacterial communities than CR, but only at pre-planting. In contrast, the stability index of fungal communities was significantly affected by rotation, with a greater stability index in SBR relative to CR (Fig. 5B; Table S3; $P < 0.05$). Subsequent Random Forest models identified bacterial and fungal alpha diversity as the most important predictors for their respective community stability (Figs. 5C and D), with a positive linear relationship between community stability and alpha diversity (Figs. 5E and F). Bacterial community composition, TN, M3 Zn, and PNM were also significantly associated with bacterial community stability (Fig. 5C), whereas resin P was significantly linked to fungal community stability (Fig. 5D).

Linking environment, soil chemical properties, and microbial communities to peanut yield

Using PLS-PM, we examined the linkages among changes in weather, irrigation, microbial communities (abundance, diversity, composition, and community stability), microbial networks (keystone taxa and complexity), soil chemical properties (important predictors for yield determined by Random Forest modeling; Fig. S4), and peanut yield. Differences in peanut yield between irrigated and rainfed conditions under different rotation systems are shown in Fig. S5.

Under CR (Fig. 6A), the increase in temperature, precipitation, and radiation showed negative impacts on bacterial communities (path coefficient = −0.67, $P < 0.01$), but positive effects on fungal communities (path coefficient = 0.43, $P < 0.05$) and the microbial network (path coefficient = 0.71, $P < 0.001$). Bacterial communities (path coefficient = −0.38, $P < 0.05$) were negatively linked to the microbial network, and these two microbial attributes (path coefficient = −0.57, $P < 0.05$; path coefficient = −0.91, $P < 0.001$) significantly and negatively impacted soil chemical properties (NH_4^+-N, POXC, C:N, TN, pH, BS, and M3 P, S and B; Fig. S4A). Irrigation (path coefficient = 0.50, $P < 0.05$) and bacterial communities (path coefficient = −0.44, $P < 0.05$) had contrasting effects on peanut yield.

Under SBR (Fig. 6B), increasing temperature, precipitation, and radiation negatively affected bacterial communities (path coefficient = −0.53, $P < 0.05$) and the latter were negatively linked to the microbial network (path coefficient = −0.99, $P < 0.001$). However, the microbial network (path coefficient = 0.54, $P < 0.05$) made a positive contribution to soil chemical properties (BS, CEC, TN, pH, PNM, TC, POXC, resin P, and M3 Ca, S, Fe and Mg; Fig. S4B). The microbial network (path coefficient = 0.49, $P < 0.05$), soil chemical properties (path coefficient = 0.77, $P < 0.001$), and bacterial communities (path coefficient = 0.76, $P < 0.001$) were significantly and positively related to peanut yield.

Discussion

Soil microbiomes play a critical role in the biogeochemical cycling of micro- and macro-nutrients that are vital for plant growth and serve as a key driver of agroecosystem functioning (Bardgett and van der Putten 2014; Crowther et al. 2019). By tracking variations in soil AMP and soil chemical properties across plant developmental stages, this study advances our fundamental understanding of the impact of long-term agricultural practices on the linkages among soil microbiomes, soil health, and crop productivity.

Sod-based rotation affected soil microbiomes and improved soil health

Crop rotation and sampling time strongly affected multiple soil microbial attributes, including diversity, community composition, and bacterial-fungal networks. The abundance of microbial communities was more sensitive to sampling time than crop rotation, implying that season-dependent effects (e.g., soil temperature, precipitation, and radiation) were a key factor shaping soil microbiomes (Lauber et al.

Table 2 Effects of irrigation, sampling time, and rotation on bacterial and fungal communities based on PERMANOVA

		Irrigation	time	Rotation	Irrigation × time	Irrigation × rotation	Time × rotation	Irrigation × time × rotation
Bacterial communities	R^2	0.04	0.10	0.09	0.05	0.02	0.05	0.04
	P	**0.02***	**< 0.001*****	**< 0.001*****	0.39	0.49	0.26	0.96
Fungal communities	R^2	0.03	0.15	0.16	0.04	0.02	0.05	0.04
	P	0.28	**< 0.001*****	**< 0.001*****	0.70	0.60	**0.09**†	0.35

***, **, *, and † indicate significance (marked in bold) at $P < 0.001$, 0.01, 0.05, and 0.1, respectively

2013; Mediavilla et al. 2020). Interestingly, bacterial diversity and microbial community dissimilarity were significantly lower at maturity, although microbial abundance was greater at maturity, irrespective of crop rotation and irrigation. This was likely due to the tight link between plants and microorganisms during plant growth, when plants trigger the rhizosphere effect (Geisen et al. 2021; Zhao et al. 2021). Specifically, plants modulate exudation patterns, metabolism, and immune-associated traits at different developmental stages based on nutrient demand and tolerance to biotic and abiotic stress (Sasse et al. 2018; Trivedi et al. 2020; Zhao et al. 2021). This ultimately tailors the assembly and turnover of microbiomes, especially bacterial communities, given that rhizodeposition is considered to be dominated by labile C inputs (Kuzyakov 2010; Mendes et al. 2014; Pausch and Kuzyakov 2018). This effect was evident

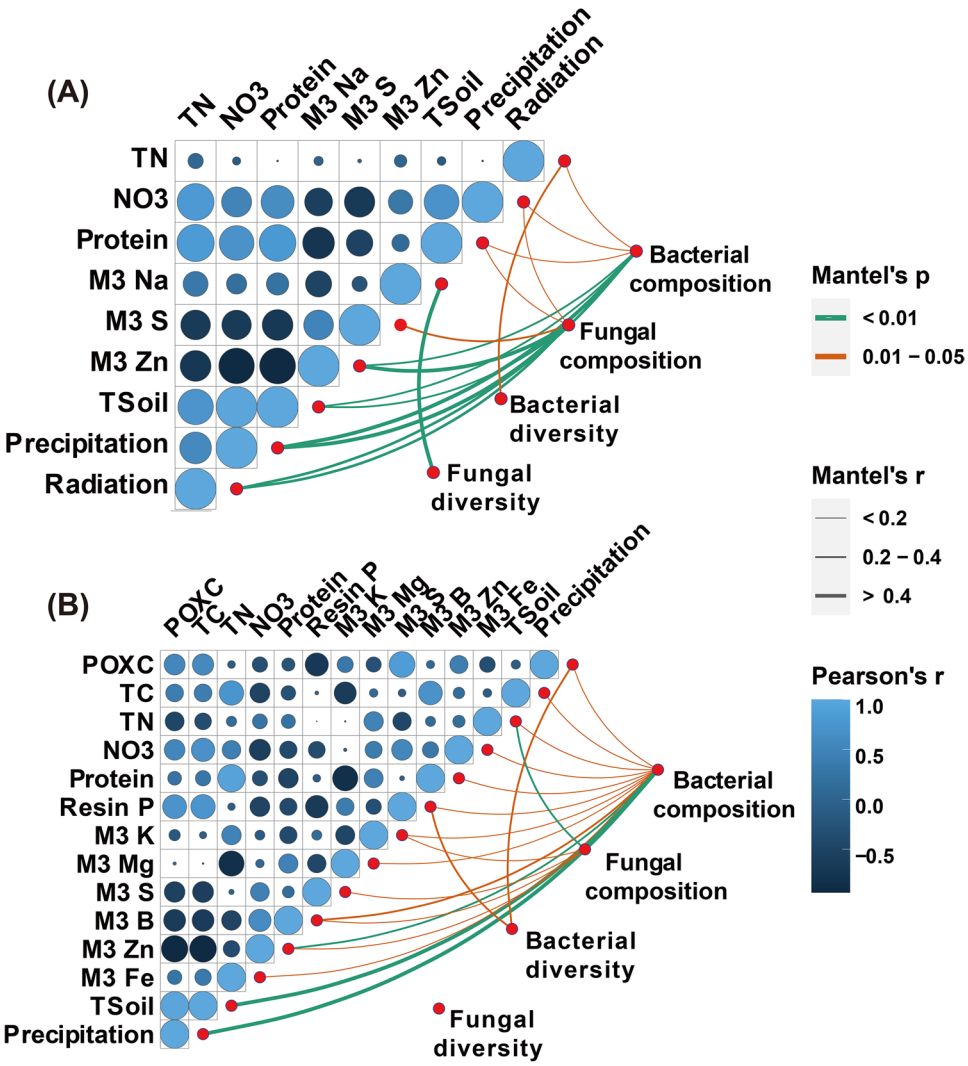

Fig. 2 Correlations between environmental factors and microbial communities under CR (**A**) and SBR (**B**). Only variables with at least one significant correlation ($P < 0.05$) under CR and/or SBR are shown. Line width is proportional to the partial Mantel's r statistic, and line color denotes the statistical significance based on 999 permutations (orange, $0.01 < P < 0.05$; green, $P < 0.01$). Pairwise comparisons of environmental factors are also shown, with a gradient of color and size of circles denoting Pearson's correlation coefficient. *P* values were adjusted for multiple testing with the Bonferroni-Holm method. POXC, permanganate-oxidizable C; TC, total C; TN, total N; Tsoil, average soil temperature; Precipitation, total precipitation; Radiation, average solar radiation; M3, extracted with Mehlich III

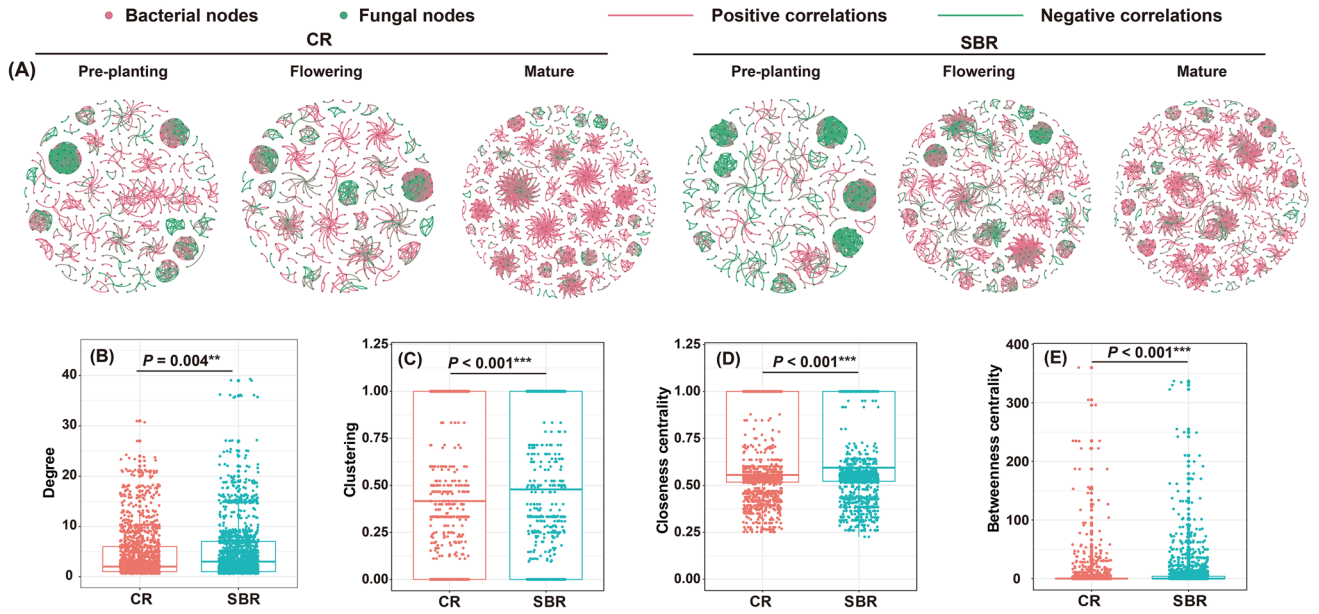

Fig. 3 **A** Bacterial-fungal co-occurrence patterns at different sampling times under CR and SBR. Each node represents an OTU, and node size is proportional to its estimated absolute abundance. The thickness of edges is proportional to their correlation coefficient, and pink and green edges represent positive and negative correlations, respectively. (**B**–**E**): Comparison of key topological properties of bacterial-fungal co-occurrence patterns (degree, clustering, closeness centrality, and betweenness centrality) that potentially determined the complexity of microbial networks across different sampling times. Specific topological properties of bacterial-fungal co-occurrence patterns at different sampling times under CR and SBR are shown in Table 3

Table 3 Topological properties of the bacterial-fungal co-occurrence networks at different developmental stages under peanut systems

	CR			SBR		
	Pre-planting	Flowering	Maturity	Pre-planting	Flowering	Maturity
Number of nodes	452	395	706	404	635	737
Bacterial nodes	310 (68.6%)	287 (72.7%)	578 (81.7%)	203 (50.2%)	467 (73.5%)	631 (85.6%)
Fungal nodes	142 (31.4%)	108 (27.3%)	128 (18.1%)	101 (49.8%)	168 (26.5%)	106 (14.4%)
Number of edges	1,043	846	1,651	1,000	1,617	1,924
Edges within bacteria	360	404	1262	205	892	1497
Edges within fungi	184	116	45	383	153	67
Edges between bacteria and fungi	399	326	344	412	572	360
Average degree	4.62	4.28	4.68	4.95	5.09	5.22
Clustering coefficient	0.86	0.71	0.67	0.90	0.67	0.89
Eigencentrality	0.07	0.06	0.05	0.07	0.06	0.05
Closeness centrality	0.74	0.62	0.64	0.75	0.72	0.75
Betweenness centrality	3.68	12.83	9.92	2.65	6.64	5.83
Average path length	1.74	2.32	2.1	1.60	2.03	1.70
Modularity	0.916	0.926	0.954	0.913	0.940	0.955
Percentage of positive correlations	89.4%	87.8%	97.4%	88.2%	79.2%	67.8%

in the SBR system, where the concentration of POXC (an indicator of "active" C) was greater at maturity compared to the other stages. Greater POXC concentrations during the peanut growing season were associated with higher bacterial abundance (Alphaproteobacteria, Bacilli, Actinobacteria, Acidobacteria-6, Thermoleophilia, Chloracidobacteria, Planctomycetia, Chloroflexi, Acidobacteriia, and Nitrospira) but lower bacterial diversity and bacterial community dissimilarity (Figs. 2B, S6A, S6C, and S6E), suggesting that this increase in a more biologically available C pool was concomitant with a homogenizing effect on the bacterial community, at least in the SBR system. Compared to fungal

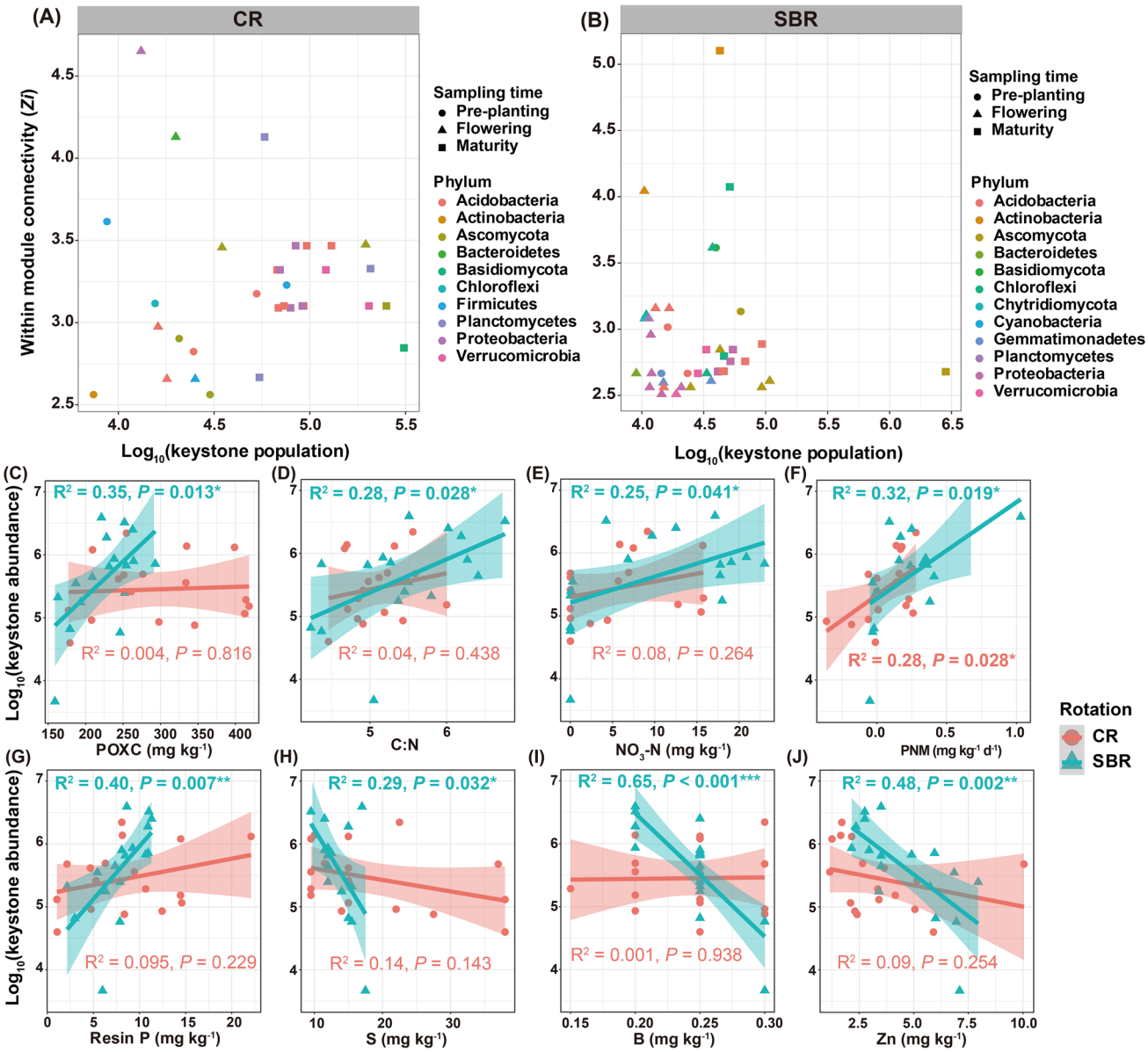

Fig. 4 The abundance of keystone taxa at different developmental stages under CR (**A**) and SBR (**B**), and associations between the abundance of keystone taxa and soil chemical properties (**C**-**J**); only properties with a significant association with either CR or SBR are presented. *P* values were adjusted by the Bonferroni-Holm method. The associations between keystone taxa and all soil chemical properties are shown in Fig. S3D. "*", "**", "***" indicate significance at $P < 0.05$, 0.01, and 0.001, respectively

diversity, bacterial diversity was more sensitive to sampling time, irrespective of rotation, consistent with previous studies in which seasonal changes had a stronger influence on bacterial relative to fungal alpha diversity (Zhang et al. 2020b). Overall, as different sampling times coincided with both season-dependent environmental changes and plant developmental stages, we cannot precisely determine the extent to which each factor made a greater contribution to structuring soil microbiomes in this study.

SBR led to higher microbial alpha diversity and distinct microbial community composition as compared to CR, consistent with our previous study based on a three-year sampling event (2017–2019) at the flowering stage under the cotton phase that found greater microbial diversity and different microbial communities in cotton roots when increasing rotational diversity by integrating bahiagrass in the SBR system (Zhang et al. 2022a). Greater temporal crop diversity may generate a legacy effect that maintains nutrient availability by retaining plant residues after harvest and releasing limiting soil nutrients, which is a key factor in structuring soil microbial communities (Tiemann et al. 2015; Furey and Tilman 2021). The significant increase in soil C measured in

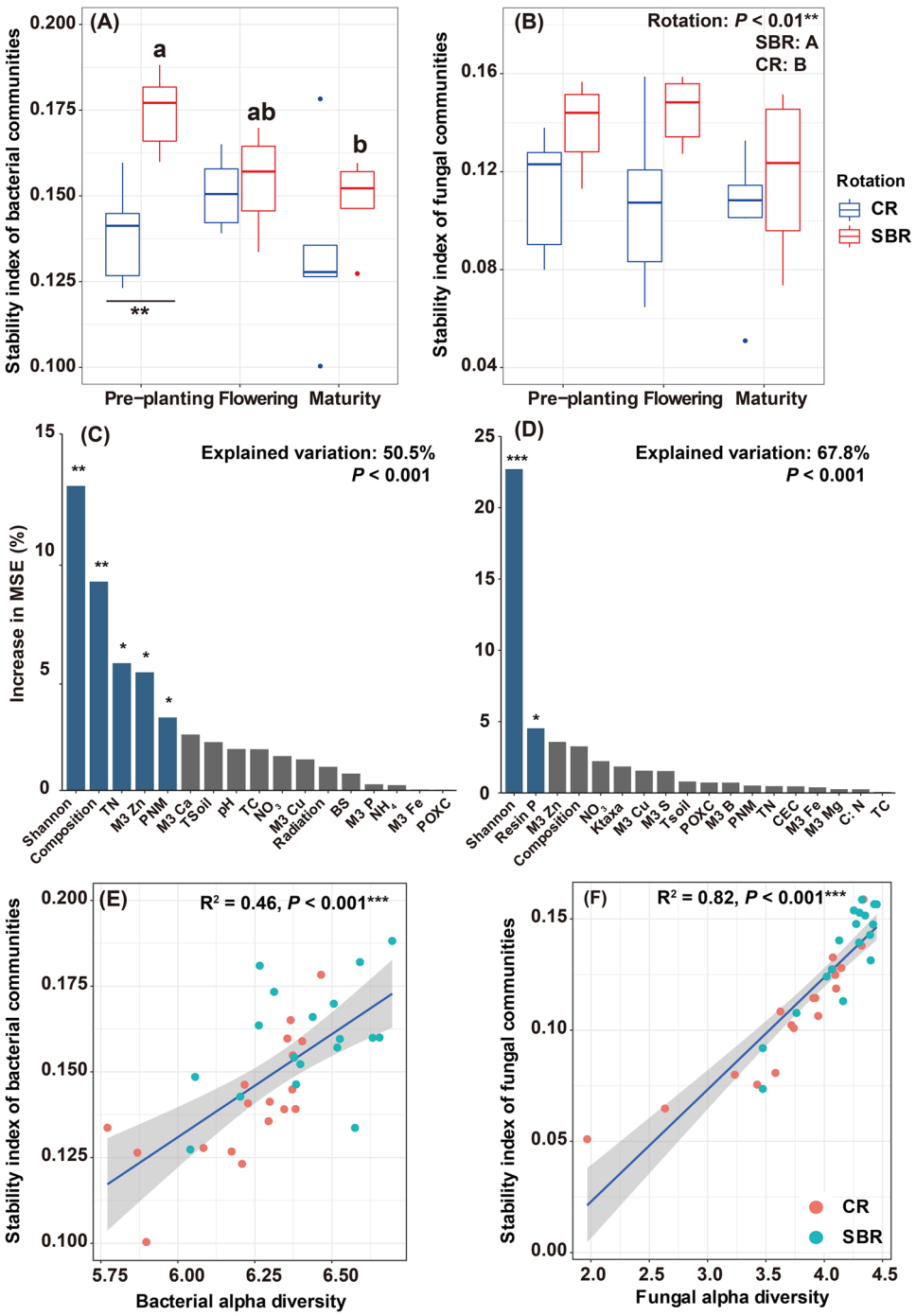

Fig. 5 Stability index of microbial communities. (A, B) stability index of bacterial (A) and fungal (B) communities at different sampling times under CR and SBR. (**A**) Lowercase letters above boxes indicate significant differences among sampling times under SBR using a one-way ANOVA followed by a Tukey's HSD test for post hoc comparisons ($P < 0.05$). Asterisks indicate significant differences between CR and SBR at pre-planting. (**B**) Uppercase letters next to rotation indicate significant differences between SBR and CR. Statistical analysis for the stability index of microbial communities is shown in Table S3. (**C**, **D**) Random Forest mean predictor importance of soil chemical and weather properties for the stability of bacterial (C) and fungal (D) community. Shannon, Shannon index; Composition, community composition as computed by first principal coordinate analysis score; Ktaxa, keystone taxa; POXC, permanganate-oxidizable C; TC, total C; TN, total nitrogen; PNM, potential nitrogen mineralization rate; CEC, cation exchange capacity; BS, base saturation; Tsoil, average soil temperature; Radiation, average solar radiation; M3, extracted with Mehlich III. (**E** and **F**) Linear relationship between alpha diversity of bacterial (E) and fungal (F) communities and their corresponding community stability index. Statistical analysis was performed using ordinary least squares linear regressions. *P* values were adjusted by the Bonferroni-Holm method. "*", "**", "***" indicate significance at $P < 0.05$, 0.01, and 0.001, respectively

SBR relative to CR is consistent with the greater crop growth and productivity observed in SBR (Zhao et al. 2009; Zhang et al. 2022a), which should increase the quantity and quality of aboveground biomass inputs due to the rotational effect (Zhang et al. 2021). More plant litter inputs can increase the activity of free-living microbes and subsequently enhance soil functioning, e.g., organic matter mineralization, C sequestration, nitrification, and P solubilization. This can facilitate nutrient availability, especially limiting elements for plant growth (e.g., N, P, Zn, and Fe), and subsequently stimulate above-belowground interactions (Steinauer et al. 2016). Furthermore, stronger above-belowground interactions should affect C allocation and rhizodeposition in SBR (Steinauer et al. 2016; Zhang et al. 2021) and intensify ecological connections between soil microbial communities and microbially-derived nutrient dynamics (Zhang et al. 2021, 2022b). This is consistent with the greater number of significant links between soil chemical properties and microbial

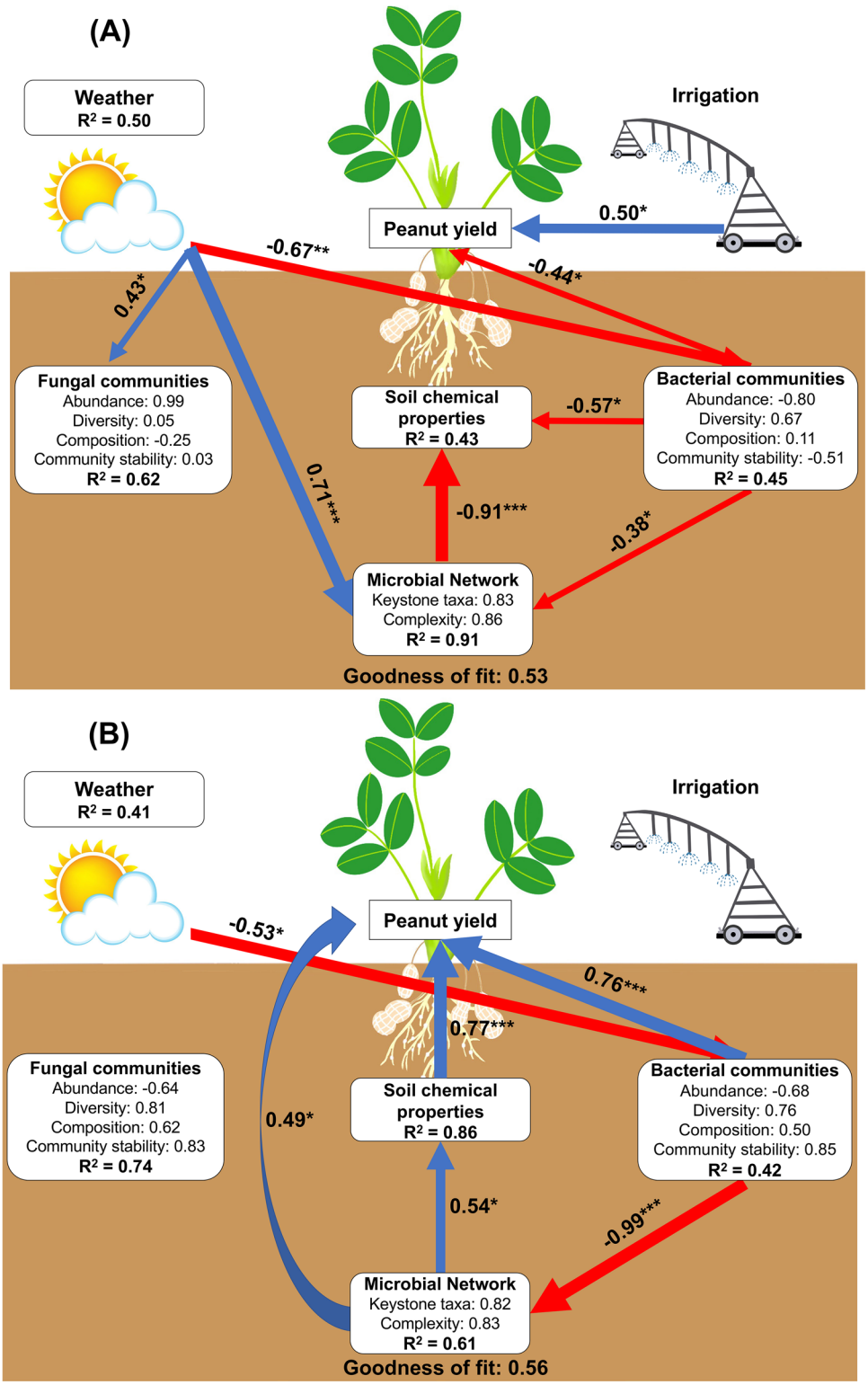

Fig. 6 Partial least squares path modeling showing cascading relationships of irrigation and weather on microbial communities, microbial network, soil chemical properties, and peanut yield under CR (**A**) and SBR (**B**). Path coefficients indicate the direction and strength of the relationships between variables while coefficients of determination (R^2) indicate the amount of variance in latent variables that is explained by the manifest variables included in their computation; both were calculated with 1000 bootstraps. Latent variables are bolded in each box and inferred from manifest variables, where values following each manifest variable indicate the strength of the relationship between this manifest variable and the latent variable. The manifest variables contributing to the latent variable soil chemical properties under CR and SBR are shown in Fig. S4. Blue and red arrows indicate positive and negative relationships, respectively. Values adjacent to arrows indicate path coefficients, and the width of arrows shows the strength of path coefficients. *, **, and *** indicate significance at $P < 0.05$, 0.01, and 0.001, respectively

community composition we observed in SBR, especially for bacterial communities, as well as higher concentrations or rates of TC, TN, NO_3^--N, PNM, resin P, and M3 Mg, Zn, Fe, and Cu. Overall, these results indicate that higher rotational diversity can stimulate C storage and improve nutrient availability and soil health through positive feedback loops between nutrient cycling and microbial attributes.

SBR had a significantly larger stability index of microbial communities than CR, implying that microbial communities in SBR were more stable. As expected, microbial diversity

made the largest contribution to microbial community stability and these strong positive relationships between diversity and community stability of soil microbiomes further support the diversity-stability hypothesis underlying plant-microbiome interactions (Wagg et al. 2018; Ratzke et al. 2020). Besides biotic factors, a subset of soil chemical properties mostly related to N was a significant contributor to bacterial community stability (Fig. 5C). Peanut can release high-quality litter and organic sources (e.g., high N concentration, low C:N and concentration of phenol and lignin) to the soil (Pan et al. 2019), profoundly affecting the activity and turnover of fast-growing microbes, such as bacterial communities (Ho et al. 2017). In turn, microbial communities can enhance N cycling processes and N transformations. We found a greater PNM rate, NO_3^--N concentration, and estimated absolute abundance of Nitrospira (a dominant nitrite oxidizer or comammox) and lower concentration of soil protein throughout the growing season under SBR, although soil protein was greater at pre-planting in SBR relative to CR (Figs. 1A and B; Table 1). This implies that soil microbial communities associated with higher rotational diversity had a greater ability to promote microbially-mediated N cycling. Besides, SBR had greater concentrations of TN and NO_3^--N at each sampling time than CR, implying that SBR with high microbially mediated N processes can ultimately increase N retention and availability. This is consistent with our previous study in the cotton crop grown after peanut in these plots, where SBR induced a significantly higher relative abundance of Nitrospira and greater concentrations of TN and NO_3^-–N relative to CR (Zhang et al. 2022b). Collectively, these results demonstrate that peanut litter or residues have greater direct and indirect effects on structuring microbial communities under SBR, where they promote microbially-mediated N dynamics and N retention.

Sod-based rotation promoted network complexity and ecological functions of keystone taxa while increasing crop productivity

SBR significantly increased the network complexity of soil microbiomes, most likely as a result of higher C and nutrient availability in SBR compared to CR. Soil microbial complexity is highly associated with resource availability (Guo et al. 2020a; Qiu et al. 2021), where resource limitation may impair microbial diversity and network complexity (Barberán et al. 2012; Banerjee et al. 2016, 2019). Notably, we found that SBR had a larger percentage of negative correlations than CR (Fig. 3A and Table 3), where negative correlations in the microbial network can be a proxy for network stability and fewer negative correlations in microbiomes may cause destabilization of microbial communities (Coyte et al. 2015; Yuan et al. 2021; Hernandez et al. 2021). This suggests that microbial communities associated with the higher rotational diversity in SBR were more stable (Yuan et al. 2021; Hernandez et al. 2021), consistent with a greater stability index of microbial communities in SBR relative to CR. It is likely that taxa involved in antagonistic interspecific interactions in CR may be replaced by slow-growing oligotrophic microbes when resources are limited (Männistö et al. 2016; Hernandez et al. 2021), as evidenced by the higher estimated absolute abundance of oligotrophic taxa (e.g., bacterial class Acidobacteriia, Alphaproteobacteria, and Deltaproteobacteria, bacterial phylum Gemmatimonadetes, and fungal phylum Basidiomycota) (Ho et al. 2017) in CR than SBR. This is consistent with our prior study in cotton plots where CR had a higher relative abundance of Alphaproteobacteria, Deltaproteobacteria, and Gemmatimonadetes compared to SBR (Zhang et al. 2022b).

We also observed a larger abundance of keystone taxa and a greater diversity of microbial phyla and genera to which they were assigned under SBR relative to CR. This suggests that SBR promoted the richness of keystone taxa that complexify the network community (Yuan et al. 2021) as keystone taxa can also act as an indicator of community shifts and compositional turnover (Herren and McMahon 2018; Banerjee et al. 2018). Keystone taxa (mainly bacterial taxa) with higher abundance and richness in SBR were associated with higher functional potential, e.g., photoautotrophy, litter decomposition, nitrification, N fixation, and S respiration and oxidation (Fig. S3C). The abundance of keystone taxa was significantly related to the concentration or rate of POXC, C:N, NO_3^--N, PNM, resin P, M3 S, B, and Zn under SBR (Figs. 4C to J), whereas there was only a single significant positive correlation between keystone taxa and PNM under CR (Fig. 4F). This demonstrates how higher richness and abundance of keystone taxa may create an environment more favorable to soil microbial composition and function and potentially promote above-belowground nutrient flows that are conducive to crop performance and productivity (Fig. 6; Zhang et al. 2021; Wang et al. 2022).

Among the keystone taxa present in both systems, Actinobacteria, an antagonistic bacteria that can release antibiotic compounds against plant pathogens (Álvarez-Pérez et al. 2017; Lee et al. 2021), were more abundant at flowering and maturity under SBR relative to CR, where Actinobacteria were only found at pre-planting (Table S4). Interestingly, some fungal keystone taxa (*Bipolaris* sp. at flowering and *Fusarium* sp. at maturity) found in CR might act as pathogens (Fig. S3), which could significantly reduce crop quality and productivity (Manamgoda et al. 2005; Li et al. 2018). For example, *F. oxysporum* and *F. solani* are primary pathogens that cause peanut root rot (Villarino et al. 2019). Thus, higher rotational diversity in SBR may control the assembly of pathogenic communities while supporting more beneficial microbes, consistent with our previous study reporting that SBR restricted the density of pathogens and

promoted beneficial microbes residing in cotton roots, e.g., Opitutaceae, Pseudonocardiaceae, Rhizobiaceae, Bacillaceae, Comamonadaceae, Serendipitaceae, and Glomeraceae (Zhang et al. 2022a). Compared to only eight fungal keystone OTUs that primarily functioned as saprotrophs across all sampling times in SBR, there were far more bacterial keystone OTUs (35 nodes) that played ecologically important roles in driving nutrient cycling (including C, N, S, Mn, and Fe) and improving plant health and fitness (Fig. S3 and Table S4). This is likely the main reason why bacterial rather than fungal communities largely contributed to peanut productivity (Fig. 6). Ultimately, more soil chemical properties predicted by the Random Forest analysis (Fig. S4) and a more complex and stable microbial network with higher abundance and richness of keystone taxa were positively associated with peanut productivity in SBR (Fig. 6). These results suggest that microbiomes found in a system with higher rotational diversity contributed to significant plant-growth promotion by maintaining multiple agroecosystem functions, including element cycling, nutrient provisioning, and pathogen control (Durán et al. 2018; Fan et al. 2021).

Irrespective of rotation, there were differences in the number and abundance of keystone OTUs among sampling times, suggesting that keystone taxa were affected by environmental changes (Qiu et al. 2021). However, changes in weather conditions driven by sampling time had a smaller impact on microbial network structure (complexity and keystone taxa) under SBR compared to CR (Fig. 6). This implies that more stable and complex microbial communities with a greater abundance of keystone taxa in SBR might be more resistant and adaptive to variations in weather changes, similar to the weaker effects of weather changes observed on soil microbial community composition in SBR relative to CR, especially in fungal communities (Fig. 2).

Conclusions

By quantifying and characterizing the temporal dynamics of soil AMP under long-term agricultural practices, this study improved our understanding of the linkages among soil microbiomes, soil health, and crop productivity. However, given that extracellular DNA from dead microbes can persist in soil for weeks to years, and that up to 40% of prokaryotic and fungal DNA remaining in the soil can be relic DNA from dead cells (Pietramellara et al. 2009; Carini et al. 2016), relic DNA extraction and amplification in PCR or qPCR could inflate soil microbial diversity and lead to wrongful estimates of relative/absolute abundances of microbial communities (Carini et al. 2016). Besides, as many microorganisms (e.g., bacteria) have multiple copies of the 16S rRNA gene in their genome, estimating 16S rRNA read counts via amplicon sequencing would cause biased cell count estimates. However, it is still difficult to correct 16S rRNA gene copy numbers in 16S rRNA gene amplicon sequencing (Louca et al. 2018; Starke et al. 2021). Therefore, to accurately track the roles of soil microbiomes in agroecosystem functions, future studies will need to determine changes in microbial gene expression temporally and/or spatially to confirm our study's main conclusions.

Overall, we found that rotation had a strong influence on multiple facets of soil microbial communities in this study, with greater diversity and community stability of soil microbiomes, complexity and stability of bacterial-fungal networks, and abundance and richness of keystone taxa in SBR relative to CR. This may make soil microbiomes more adaptive and resilient to weather variability. Compared to CR, SBR exhibited greater concentrations of TC, TN, NO_3^--N, resin P, M3 Mg, Zn, Fe, and Cu, along with greater PNM rates and C:N ratio. Also, there were more significant links between soil chemical properties and microbial community composition and the abundance of keystone taxa under SBR. These suggest that higher rotational diversity can intensify ecological connections among soil, microbes, and plants and further enhance agroecosystem functions, including increasing soil C storage and improving nutrient availability and soil health. Finally, a greater number of bacterial keystone OTUs were linked to nutrient cycling and improvements in plant health and fitness compared to fungal keystone OTUs under SBR. Overall, this study provided new insights on soil-microbes-plant interactions underlying high rotational diversity and shed light on the importance of diversifying rotational diversity to enhance soil health, soil microbial attributes, and crop productivity.

Supplementary Information The online version contains supplementary material available at https://doi.org/10.1007/s00374-022-01675-4.

Acknowledgements We thank Lesley Schumacher for her help in collecting soil samples, Sudeep S. Sidhu for helping to harvest and determine peanut productivity, and Angelique Bochnak for sample analysis for soil protein. We also thank the staff at the North Florida Research and Education Center for the maintenance of the long-term field site at Quincy.

Funding This work was financially supported by a United States Department of Agriculture (USDA)-Southern Sustainable Agriculture Research and Education (SSARE) grant award (2017–38640-26914) to H.-L. Liao, a USDA-NIFA (2019–67013-29107) award to H.-L. Liao, a USDA-SSARE (2019–38640-29878, SUB00002463) grant award to H.-L. Liao and K. Zhang, a USDA-NIFA Hatch project (FLA-SWS-005733) to G. Maltais-Landry, UF Graduate School Funding Awards to K. Zhang and M. James, and 2021–2022 Peanut Check-off funds to H.-L. Liao, G. Maltais-Landry and K. Zhang.

Declarations

Ethics approval Not applicable.

Consent to participate Not applicable.

Consent for publication All authors have approved the manuscript in its entirety and agreed for its publication.

Conflict of interest The authors declare no competing interests.

References

Allar J, Maltais-Landry G (2022) Limited benefits of summer cover crops on nitrogen cycling in organic vegetable production. Nutr Cycling Agroecosyst 122:119–138

Almeida A, Shao Y (2018) Genome watch: keeping tally in the microbiome. Nat Rev Microbiol 16:124

Álvarez-Pérez JM, González-García S, Cobos R, Olego MÁ, Ibañez A, Díez-Galán A, Garzón-Jimeno E, Coque JJ (2017) Use of endophytic and rhizosphere actinobacteria from grapevine plants to reduce nursery fungal graft infections that lead to young grapevine decline. Appl Environ Microbiol 83:e01564-e1617

Badri DV, Vivanco JM (2009) Regulation and function of root exudates. Plant Cell Environ 32:666–681

Banerjee S, Kirkby CA, Schmutter D, Bissett A, Kirkegaard JA, Richardson AE (2016) Network analysis reveals functional redundancy and keystone taxa amongst bacterial and fungal communities during organic matter decomposition in an arable soil. Soil Biol Biochem 97:188–198

Banerjee S, Schlaeppi K, van der Heijden MGA (2018) Keystone taxa as drivers of microbiome structure and functioning. Nat Rev Microbiol 16:567–576

Banerjee S, Walder F, Büchi L, Meyer M, Held AY, Gattinger A, Keller T, Charles R, van der Heijden MG (2019) Agricultural intensification reduces microbial network complexity and the abundance of keystone taxa in roots. ISME J 13:1722–1736

Barberán A, Bates ST, Casamayor EO, Fierer N (2012) Using network analysis to explore co-occurrence patterns in soil microbial communities. ISME J 6:343–351

Barberán A, Ramirez KS, Leff JW, Bradford MA, Wall DH, Fierer N (2014) Why are some microbes more ubiquitous than others? Predicting the habitat breadth of soil bacteria. Ecol Lett 17:794–802

Bardgett RD, van der Putten WH (2014) Belowground biodiversity and ecosystem functioning. Nature 515:505–511

Bastian M, Heymann S, Jacomy M (2009) Gephi: an open source software for exploring and manipulating networks. ICWSM 3:361–362

Bender SF, Wagg C, van der Heijden MGA (2016) An underground revolution: biodiversity and soil ecological engineering for agricultural sustainability. Trends Ecol Evol 31:440–452

Benjamini Y, Hochberg Y (1995) Controlling the false discovery rate: a practical and powerful approach to multiple testing. J R Stat Soc B 57:289–300

Berendsen RL, Pieterse CMJ, Bakker PAHM (2012) The rhizosphere microbiome and plant health. Trends Plant Sci 17:478–486

Bolyen E, Rideout JR, Dillon MR, Bokulich NA, Abnet CC, Al-Ghalith GA, Alexander H, Alm EJ, Arumugam M, Asnicar F, Bai Y (2019) Reproducible, interactive, scalable and extensible microbiome data science using QIIME 2. Nat Biotechnol 37:852–857

Bommarco R, Kleijn D, Potts SG (2013) Ecological intensification: harnessing ecosystem services for food security. Trends Ecol Evol 28:230–238

Brabcová V, Nováková M, Davidová A, Baldrian P (2016) Dead fungal mycelium in forest soil represents a decomposition hotspot and a habitat for a specific microbial community. New Phytol 210:1369–1381

Breiman L (2001) Random forests. Mach Learn 45:5–32

Campbell BM, Beare DJ, Bennett EM, Hall-Spencer JM, Ingram JS, Jaramillo F, Ortiz R, Ramankutty N, Sayer JA, Shindell D (2017) Agriculture production as a major driver of the Earth system exceeding planetary boundaries. Ecol Soc 22:8

Carini P, Marsden PJ, Leff JW et al (2016) Relic DNA is abundant in soil and obscures estimates of soil microbial diversity. Nat Microbiol 2:16242

Chen K-H, Longley R, Bonito G, Liao H-L (2021) A two-step PCR protocol enabling flexible primer choice and high sequencing yield for Illumina MiSeq Meta-Barcoding. Agronomy 11:1274

Coyte KZ, Schluter J, Foster KR (2015) The ecology of the microbiome: networks, competition, and stability. Science 350:663–666

Crowther TW, van den Hoogen J, Wan J, Mayes MA, Keiser AD, Mo L, Averill C, Maynard DS (2019) The global soil community and its influence on biogeochemistry. Science 365:aav0550

Culman SW, Snapp SS, Freeman MA, Schipanski ME, Beniston J, Lal R, Drinkwater LE, Franzluebbers AJ, Glover JD, Grandy AS, Lee J (2012) Permanganate oxidizable carbon reflects a processed soil fraction that is sensitive to management. Soil Sci Soc Am J 76:494–504

D'Hondt K, Kostic T, McDowell R, Eudes F, Singh BK, Sarkar S, Markakis M, Schelkle B, Maguin E, Sessitsch A (2021) Microbiome innovations for a sustainable future. Nat Microbiol 6:138–142

de Vries FT, Griffiths RI, Bailey M, Craig H, Girlanda M, Gweon HS, Hallin S, Kaisermann A, Keith AM, Kretzschmar M, Lemanceau P (2018) Soil bacterial networks are less stable under drought than fungal networks. Nat Commun 9:3033

Doane TA, Horwáth WR (2003) Spectrophotometric determination of nitrate with a single reagent. Anal Lett 36:2713–2722

Durán P, Thiergart T, Garrido-Oter R, Agler M, Kemen E, Schulze-Lefert P, Hacquard S (2018) Microbial interkingdom interactions in roots promote arabidopsis survival. Cell 175:973-983.e14

Eisenhauer N, Lanoue A, Strecker T, Scheu S, Steinauer K, Thakur MP, Mommer L (2017) Root biomass and exudates link plant diversity with soil bacterial and fungal biomass. Sci Rep 7:44641

Fan K, Delgado-Baquerizo M, Guo X, e Guo X, Wang D, Zhu YG, Chu H (2021) Biodiversity of key-stone phylotypes determines crop production in a 4-decade fertilization experiment. ISME J 15:550–561

Faucon M-P, Houben D, Lambers H (2017) Plant functional traits: soil and ecosystem services. Trends Plant Sci 22:385–394

Faust K, Raes J (2012) Microbial interactions: from networks to models. Nat Rev Microbiol 10:538–550

Foley JA, Ramankutty N, Brauman KA, Cassidy ES, Gerber JS, Johnston M, Mueller ND, O'Connell C, Ray DK, West PC, Balzer C (2011) Solutions for a cultivated planet. Nature 478:337–342

Fortmann-Roe S, Others, (2015) Consistent and clear reporting of results from diverse modeling techniques: the A3 method. J Stat Softw 66:1–23

Fuhrman JA (2009) Microbial community structure and its functional implications. Nature 459:193–199

Furey GN, Tilman D (2021) Plant biodiversity and the regeneration of soil fertility. Proc Natl Acad Sci USA 118

Gastwirth JL, Gel YR, Miao W (2009) The impact of Levene's test of equality of variances on statistical theory and practice. Stat Sci 24:343–360

Geisen S, Heinen R, Andreou E, van Lent T, Ten Hooven FC, Thakur MP (2021) Contrasting effects of soil microbial interactions on growth–defence relationships between early- and mid-successional plant communities. New Phytol 233:1345–1357

Guo J, Ling N, Chen Z, Xue C, Li L, Liu L, Gao L, Wang M, Ruan J, Guo S, Vandenkoornhuyse P (2020) Soil fungal assemblage complexity is dependent on soil fertility and dominated by deterministic processes. New Phytol 226:232–243

Guo X, Zhang X, Qin Y, Liu YX, Zhang J, Zhang N, Wu K, Qu B, He Z, Wang X, Zhang X (2020) Host-associated quantitative abundance profiling reveals the microbial load variation of root microbiome. Plant Commun 1:100003

Hanusz Z, Tarasińska J (2015) Normalization of the Kolmogorov-Smirnov and Shapiro-Wilk tests of normality. Biom Lett 52:85–93

Hartman K, van der Heijden MGA, Wittwer RA, Banerjee S, Walser JC, Schlaeppi K (2018) Cropping practices manipulate abundance patterns of root and soil microbiome members paving the way to smart farming. Microbiome 6:14

Haskett TL, Tkacz A, Poole PS (2020) Engineering rhizobacteria for sustainable agriculture. ISME J 15:949–964

Hector A (2015) The new statistics with R: an introduction for biologists. Oxford University Press

Hernandez DJ, David AS, Menges ES, Searcy CA, Afkhami ME (2021) Environmental stress destabilizes microbial networks. ISME J 15:1722–1734

Herren CM, McMahon KD (2018) Keystone taxa predict compositional change in microbial communities. Environ Microbiol 20:2207–2217

Ho A, Di Lonardo DP, Bodelier PLE (2017) Revisiting life strategy concepts in environmental microbial ecology. FEMS Microbiol Ecol 93:fix006

Hurisso TT, Culman SW, Zhao K (2018) Repeatability and spatiotemporal variability of emerging soil health indicators relative to routine soil nutrient tests. Soil Sci Soc Am J 82:939–948

Hurisso TT, Moebius-Clune DJ, Culman SW, Moebius-Clune BN, Thies JE, van Es HM (2018) Soil protein as a rapid soil health indicator of potentially available organic nitrogen. Agric Environ Lett 3:180006

Jiao S, Lu Y, Wei G (2022) Soil multitrophic network complexity enhances the link between biodiversity and multifunctionality in agricultural systems. Glob Chang Biol 28:140–153

Kemmitt SJ, Wright D, Jones DL (2005) Soil acidification used as a management strategy to reduce nitrate losses from agricultural land. Soil Biol Biochem 37:867–875

Kuzyakov Y (2010) Priming effects: Interactions between living and dead organic matter. Soil Biol Biochem 42:1363–1371

Lauber CL, Ramirez KS, Aanderud Z, Lennon J, Fierer N (2013) Temporal variability in soil microbial communities across land-use types. ISME J 7:1641–1650

Lee S-M, Kong HG, Song GC, Ryu C-M (2021) Disruption of Firmicutes and Actinobacteria abundance in tomato rhizosphere causes the incidence of bacterial wilt disease. ISME J 15:330–347

Li X, de Boer W, Ding C, Zhang T, Wang X (2018) Suppression of soil-borne Fusarium pathogens of peanut by intercropping with the medicinal herb Atractylodes lancea. Soil Biol Biochem 116:120–130

Louca S, Parfrey LW, Doebeli M (2016) Decoupling function and taxonomy in the global ocean microbiome. Science 353:1272–1277

Louca S, Doebeli M, Parfrey LW (2018) Correcting for 16S rRNA gene copy numbers in microbiome surveys remains an unsolved problem. Microbiome 6:1–12

Manamgoda DS, Rossman AY, Castlebury LA, Crous PW, Madrid H, Chukeatirote E, Hyde KD (2005) The genus bipolaris. Stud Mycol 53:173–189

Männistö M, Ganzert L, Tiirola M, Häggblom MM, Stark S (2016) Do shifts in life strategies explain microbial community responses to increasing nitrogen in tundra soil? Soil Biol Biochem 96:216–228

Mediavilla O, Geml J, Olaizola J, Baldrian P, López-Mondejar R, Oria-de-Rueda JA, Martín-Pinto P (2020) Seasonal influences on bacterial community dynamics in Mediterranean pyrophytic ecosystems. For Ecol Manage 478:118520

Mehlich A (1984) Mehlich 3 soil test extractant: a modification of Mehlich 2 extractant. Commun Soil Sci Plant Anal 15:1409–1416

Mendes LW, Kuramae EE, Navarrete AA, Van Veen JA, Tsai SM, l, (2014) Taxonomical and functional microbial community selection in soybean rhizosphere. ISME J 8:1577–1587

Moebius-Clune BN, Es HM, Idowu OJ, Schindelbeck RR, Moebius-Clune DJ, Wolfe DW, Abawi GS, Thies JE, Gugino BK, Lucey R (2008) Long-term effects of harvesting maize Stover and tillage on soil quality. Soil Sci Soc Am J 72:960–969

Morriën E, Hannula SE, Snoek LB, Helmsing NR, Zweers H, De Hollander M, Soto RL, Bouffaud ML, Buée M, Dimmers W, Duyts H (2017) Soil networks become more connected and take up more carbon as nature restoration progresses. Nat Commun 8:14349

Nannipieri P, Paul E (2009) The chemical and functional characterization of soil N and its biotic components. Soil Biol Biochem 41:2357–2369

Pan Z, Zhang R, Zicari S (2019) Integrated processing technologies for food and agricultural by-products. Academic Press, London

Paul E (2014) Soil microbiology, ecology and biochemistry. Academic Press, London

Pausch J, Kuzyakov Y (2018) Carbon input by roots into the soil: quantification of rhizodeposition from root to ecosystem scale. Glob Chang Biol 24:1–12

Pietramellara G, Ascher J, Borgogni F, Ceccherini MT, Guerri G, Nannipieri P (2009) Extracellular DNA in soil and sediment: fate and ecological relevance. Biol Fertil Soils 45:219–235

Põlme S, Abarenkov K, Henrik Nilsson R, Lindahl BD, Clemmensen KE, Kauserud H, Nguyen N, Kjøller R, Bates ST, Baldrian P, Frøslev TG (2020) FungalTraits: a user-friendly traits database of fungi and fungus-like stramenopiles. Fungal Divers 105:1–16

Props R, Kerckhof F-M, Rubbens P, De Vrieze J, Hernandez Sanabria E, Waegeman W, Monsieurs P, Hammes F, Boon N (2017) Absolute quantification of microbial taxon abundances. ISME J 11:584–587

Qiu L, Zhang Q, Zhu H, Reich PB, Banerjee S, van der Heijden MG, Sadowsky MJ, Ishii S, Jia X, Shao M, Liu B (2021) Erosion reduces soil microbial diversity, network complexity and multifunctionality. ISME J 15:2474–2489

Ratzke C, Barrere J, Gore J (2020) Strength of species interactions determines biodiversity and stability in microbial communities. Nat Ecol Evol 4:376–383

Sasse J, Martinoia E, Northen T (2018) Feed your friends: do plant exudates shape the root microbiome? Trends Plant Sci 23:25–41

Shen C, He J-Z, Ge Y (2021) Seasonal dynamics of soil microbial diversity and functions along elevations across the treeline. Sci Total Environ 794:148644

Shi S, Nuccio EE, Shi ZJ, He Z, Zhou J, Firestone MK (2016) The interconnected rhizosphere: high network complexity dominates rhizosphere assemblages. Ecol Lett 19:926–936

Simon E, Canarini A, Martin V, Séneca J, Böckle T, Reinthaler D, Pötsch EM, Piepho HP, Bahn M, Wanek W, Richter A (2020) Microbial growth and carbon use efficiency show seasonal responses in a multifactorial climate change experiment. Commun Biol 3:584

Starke R, Pylro VS, Morais DK (2021) 16S rRNA gene copy number normalization does not provide more reliable conclusions in metataxonomic surveys. Microb Ecol 81:535–539

Steinauer K, Chatzinotas A, Eisenhauer N (2016) Root exudate cocktails: the link between plant diversity and soil microorganisms? Ecol Evol 6:7387–7396

Tamburini G, Bommarco R, Wanger TC, Kremen C, van der Heijden MG, Liebman M, Hallin S (2020) Agricultural diversification

promotes multiple ecosystem services without compromising yield. Sci Adv 6:eaba1715
Tenenhaus M, Vinzi VE, Chatelin Y-M, Lauro C (2005) PLS path modeling. Comput Stat Data Anal 48:159–205
Tettamanti Boshier FA, Srinivasan S, Lopez A, e Hoffman NG, Proll S, Fredricks DN, Schiffer JT (2020) Complementing 16S rRNA gene amplicon sequencing with total bacterial load to infer absolute species concentrations in the vaginal microbiome. Systems 5:00777–19
Tiemann LK, Grandy AS, Atkinson EE, Marin-Spiotta E, McDaniel MD (2015) Crop rotational diversity enhances belowground communities and functions in an agroecosystem. Ecol Lett 18:761–771
Tiessen H, Moir JO (2007) Characterization of available P by sequential extraction. In: Cartar MR (ed) Soil Sampling and Methods of Analysis. Lewis Publishers, Boca Raton, FL, pp 75–86
Tkacz A, Hortala M, Poole PS (2018) Absolute quantitation of microbiota abundance in environmental samples. Microbiome 6:1–13
Trivedi P, Delgado-Baquerizo M, Trivedi C, Hu H, Anderson IC, Jeffries TC, Zhou J, Singh BK (2016) Microbial regulation of the soil carbon cycle: evidence from gene-enzyme relationships. ISME J 10:2593–2604
Trivedi P, Leach JE, Tringe SG, Sa T, Singh BK (2020) Plant-microbiome interactions: from community assembly to plant health. Nat Rev Microbiol 18:607–621
Tsiafouli MA, Thébault E, Sgardelis SP, De Ruiter PC, Van Der Putten WH, Birkhofer K, Hemerik L, De Vries FT, Bardgett RD, Brady MV, Bjornlund L (2015) Intensive agriculture reduces soil biodiversity across Europe. Glob Chang Biol 21:973–985
Villarino M, De la Lastra E, Basallote-Ureba MJ et al (2019) Characterization of Fusarium solani populations associated with spanish strawberry crops. Plant Dis 103:1974–1982
Wagg C, Dudenhöffer J-H, Widmer F, Heijden MGA (2018) Linking diversity, synchrony and stability in soil microbial communities. Funct Ecol 32:1280–1292
Wang W, Luo X, Chen Y, Ye X, Wang H, Cao Z, Ran W, Cui Z (2019) Succession of composition and function of soil bacterial communities during key rice growth stages. Front Microbiol 10:421
Wang JL, Liu KL, Zhao XQ, Gao GF, Wu YH, Shen RF (2022) Microbial keystone taxa drive crop productivity through shifting aboveground-belowground mineral element flows. Sci Total Environ 811:152342
Weatherburn MW (1967) Phenol-hypochlorite reaction for determination of ammonia. Anal Chem 39:971–974
Widder S, Allen RJ, Pfeiffer T, Curtis TP, Wiuf C, Sloan WT, Cordero OX, Brown SP, Momeni B, Shou W, Kettle H (2016) Challenges in microbial ecology: building predictive understanding of community function and dynamics. ISME J 10:2557–2568
Xia Y, Sun J, Chen DG (2018) Statistical analysis of microbiome data with R. Springer Singapore, Singapore
Xun W, Liu Y, Li W, Ren Y, Xiong W, Xu Z, Zhang N, Miao Y, Shen Q, Zhang R (2021) Specialized metabolic functions of keystone taxa sustain soil microbiome stability. Microbiome 9:1–15
Yuan MM, Guo X, Wu L, Zhang YA, Xiao N, Ning D, Shi Z, Zhou X, Wu L, Yang Y, Tiedje JM (2021) Climate warming enhances microbial network complexity and stability. Nat Clim Chang 11:343–348
Zhang F, Chen X, Vitousek P (2013) Chinese agriculture: an experiment for the world. Nature 497:33–35
Zhang K, Chen L, Li Y, Brookes PC, Xu J, Luo Y (2017) The effects of combinations of biochar, lime, and organic fertilizer on nitrification and nitrifiers. Biol Fertil Soils 53:77–87
Zhang K, Chen L, Li Y, Brookes PC, Xu J, Luo Y (2020) Interactive effects of soil pH and substrate quality on microbial utilization. Eur J Soil Biol 96:103151
Zhang K, Delgado-Baquerizo M, Zhu Y-G, Chu H (2020) Space is more important than season when shaping soil microbial communities at a large spatial scale. mSystems 5:00783–19
Zhang K, Maltais-Landry G, Liao H-L (2021) How soil biota regulate C cycling and soil C pools in diversified crop rotations. Soil Biol Biochem 156:108219
Zhang K, Maltais-Landry G, George S, Grabau ZJ, Small IM, Wright D, Liao HL (2022) Long-term sod-based rotation promotes beneficial root microbiomes and increases crop productivity. Biol Fertil Soils 58:403–419
Zhang K, Schumacher L, Maltais-Landry G, Grabau ZJ, George S, Wright D, Small IM, Liao HL (2022) Integrating perennial bahiagrass into the conventional rotation of cotton and peanut enhances interactions between microbial and nematode communities. Appl Soil Ecol 170:104254
Zhang M, Zhang L, Huang S, Li W, Zhou W, Philippot L, Ai C (2022) Assessment of spike-AMP and qPCR-AMP in soil microbiota quantitative research. Soil Biol Biochem 166:108570
Zhao D, Wright DL, Marois JJ (2009) Peanut yield and grade responses to timing of bahiagrass termination and tillage in a sod-based crop rotation. Peanut Sci 36:196–203
Zhao D, Wright DL, Marois JJ, Mackowiak CL, Brennan M (2010) Improved growth and nutrient status of an oat cover crop in sod-based versus conventional peanut-cotton rotations. Agron Sustain Dev 30:497–504
Zhao M, Zhao J, Yuan J, Hale L, Wen T, Huang Q, Vivanco JM, Zhou J, Kowalchuk GA, Shen Q, l, (2021) Root exudates drive soil-microbe-nutrient feedbacks in response to plant growth. Plant Cell Environ 44:613–628